Structural Engineering and Mechanics; Vol. 1, No. 1 (1993) 87–102
DOI: http://dx.doi.org/10.12989/sem.1993.1.1.087

Geometrically non-linear transient C° finite element analysis of composite and sandwich plates with a refined theory

J.R. Kommineni† and T. Kant‡

Department of Civil Engineering, Indian Institute of Technology, Powai, Bombay-400 076, India

Abstract. A C° continuous finite element formulation of a higher order displacement theory is presented for predicting linear and geometrically non-linear in the sense of von Karman transient responses of composite and sandwich plates. The displacement model accounts for non-linear cubic variation of tangential displacement components through the thickness of the laminate and the theory requires no shear correction coefficients. In the time domain, the explicit central difference integrator is used in conjunction with the special mass matrix diagonalization scheme which conserves the total mass of the element and includes effects due to rotary inertia terms. The parametric effects of the time step, finite element mesh, lamination scheme and orthotropy on the linear and geometrically non-linear responses are investigated. Numerical results for central transverse deflection, stresses and stress resultants are presented for square/rectangular composite and sandwich plates under various boundary conditions and loadings and these are compared with the results from other sources. Some new results are also tabulated for future reference.

Key words: plates; elastic plates; composite plates; sandwich plates; shear-deformable theory; refined theory; higher-order theory; finite element analysis; large deflection analysis; geometrically non-linear analysis; transient dynamics; dynamics.

1. Introduction

In recent years, due to the increased use of composite materials in the aerospace and automotive industries because of their superior mechanical properties such as high stiffness per unit weight, high strength per unit weight and potentially low unit cost, a need has arisen for a basic understanding of their response to dynamic loading. Because of high modulus and high strength properties that composites have, structural composites undergo large deformation before they become in-elastic. Therefore, an accurate prediction of transient responses is possible only when one accounts for geometric non-linearity. Hence, studies involving the assessment of geometrically non-linear transient response of composite and sandwich laminates are receiving much attention by composite structural designers.

Geometrically non-linear analysis of isotropic plates was considered by Hinton (1976), Pica and Hinton (1980) and Akay (1980). Hinton et al. used the Reissner-Mindlin element while Akay used a mixed finite element in their works. Reddy (1983) and Nosier and Reddy (1991) presented first order and third order shear deformation theories for predicting the geo-

† Research Scholar
‡ Professor; to whom all communications should be addressed

metrically non-linear transient responses of composite layered orthotropic plates. However, the third order formulation did not include any numerical results in the non-linear context.

To the authors knowledge, investigations for predicting the dynamic linear and geometric non-linear transient response of composite and sandwich laminates are scarce. To fill this gap, in this paper, a third order shear deformation theory is constructed. In addition to the higher order shear deformation theory, a first order shear deformation theory with five degrees of freedom per node is also developed so as to enable the comparison of present formulation with a parallel formulation both for composite and sandwich laminates. Several examples drawn from the literature are analyzed and appropriate comparisons are made to show the simplicity, validity and accuracy of the present formulation.

2. Theoretical background

A composite laminate consisting of laminas with isotropic/orthotropic material properties oriented arbitrarily is considered (see Fig. 1). In present theory, the displacement components of a generic point in the laminate are assumed to be of the form,

$$
\begin{aligned}
u(x,y,z,t) &= u_o(x,y,t) + z\,\theta_x(x,y,t) + z^2\,u_o^*(x,y,t) + z^3\,\theta_x^*(x,y,t) \\
v(x,y,z,t) &= v_o(x,y,t) + z\,\theta_y(x,y,t) + z^2\,v_o^*(x,y,t) + z^3\,\theta_y^*(x,y,t) \\
w(x,y,z,t) &= w_o(x,y,t)
\end{aligned}
\tag{1}
$$

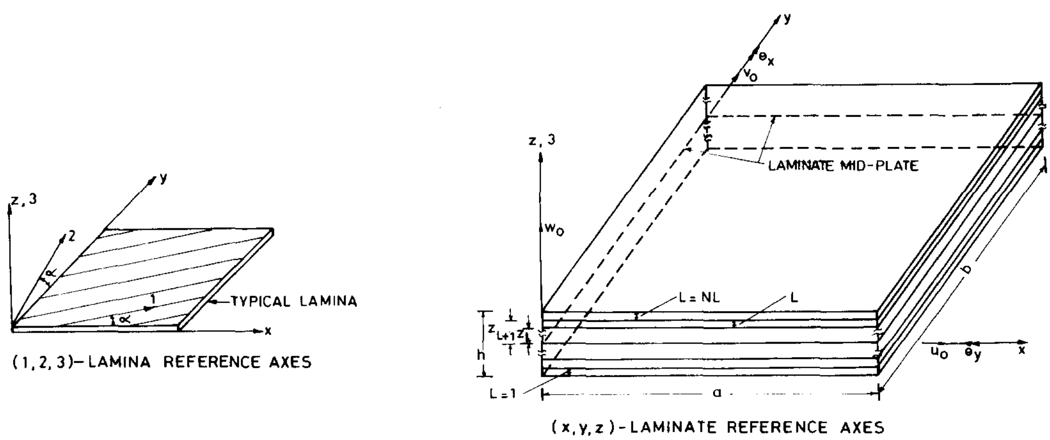

Fig. 1 Laminate geometry with positive set of lamina/laminate reference axes, displacement components and fibre orientation

where t denotes the time, u_o, v_o and w_o are the components of mid-plane displacements of a generic point having displacements u, v and w in x, y and z directions respectively. The parameters θ_x and θ_y are rotations of the transverse normal cross section in the xz and yz planes respectively. The parameters u_o^*, v_o^*, θ_x^* and θ_y^* are corresponding higher order terms in Taylor's series expansion and also defined at the mid-plane. A total Lagrangian approach is adapted and stress and strain descriptions used are those due to Piola-Kirchhoff and Green respectively. In the present context large displacements in the sense of von Karman is considered here. Then the following are the Green-Lagrangian strain displacement relations,

$$\varepsilon_x = \frac{\partial u}{\partial x} + \frac{1}{2}\left[\frac{\partial w}{\partial x}\right]^2$$

$$\varepsilon_y = \frac{\partial v}{\partial y} + \frac{1}{2}\left[\frac{\partial w}{\partial y}\right]^2$$

$$\gamma_{xy} = \frac{\partial u}{\partial y} + \frac{\partial v}{\partial x} + \frac{\partial w}{\partial x}\frac{\partial w}{\partial y}$$

$$\gamma_{yz} = \frac{\partial v}{\partial z} + \frac{\partial w}{\partial y}$$

$$\gamma_{zx} = \frac{\partial u}{\partial z} + \frac{\partial w}{\partial x} \tag{2}$$

To develop the equations of motion of the composite and sandwich laminate, the Hamilton's variational principle is used here. According to Hamilton's variational principle, the first variation of the Lagrangian function must vanish, if $L_f = \Pi - E$

$$\delta \int_{t_1}^{t_2} L_f \, dt = 0 \tag{3}$$

where δ is variation taken during indicated time interval and integral of L_f takes an extreme value which can be shown to be a minimum. The parameters E and Π defines the kinetic and potential energies of the system, respectively.

The simplified mathematical statement of Hamilton's variational principle can be written as

$$\int_{t_1}^{t_2} (\delta U - \delta W - \delta E)\, dt = 0 \tag{4}$$

where δU, δE and δW are the first variations of strain energy, kinetic energy and the work done by the external loads respectively. By substituting the expressions for strain components in above functional while carrying out the explicit integration through the laminate thickness leads to the definition of stress resultant vector $\bar{\sigma}$ and is explained as follows

$$\bar{\boldsymbol{\sigma}} = (N_x, N_y, N_{xy}, N_x^*, N_y^*, N_{xy}^*, M_x, M_y, M_{xy}, M_x^*, M_y^*, M_{xy}^*, Q_x, Q_y, Q_x^*, Q_y^*, S_x, S_y)^t$$

in which, (5a)

$$\begin{bmatrix} N_x & N_x^* \\ N_y & N_y^* \\ N_{xy} & N_{xy}^* \end{bmatrix} = \sum_{L=1}^{NL} \int_{z_L}^{z_{L+1}} \begin{bmatrix} \sigma_x \\ \sigma_y \\ \tau_{xy} \end{bmatrix} [1, z^2]\, dz$$

$$\begin{bmatrix} M_x & M_x^* \\ M_y & M_y^* \\ M_{xy} & M_{xy}^* \end{bmatrix} = \sum_{L=1}^{NL} \int_{z_L}^{z_{L+1}} \begin{bmatrix} \sigma_x \\ \sigma_y \\ \tau_{xy} \end{bmatrix} [z, z^3]\, dz$$

$$\begin{bmatrix} Q_x & Q_x^* & S_x \\ Q_y & Q_y^* & S_y \end{bmatrix} = \sum_{L=1}^{NL} \int_{z_L}^{z_{L+1}} \begin{bmatrix} \tau_{xz} \\ \tau_{yz} \end{bmatrix} [1, z^2, z]\, dz \tag{5b}$$

where $\boldsymbol{\sigma}^t = [\sigma_x, \sigma_y, \tau_{xy}, \tau_{xz}, \tau_{yz}]$ and $\boldsymbol{\varepsilon}^t = [\varepsilon_x, \varepsilon_y, \gamma_{xy}, \gamma_{xz}, \gamma_{yz}]$ are respectively vectors of stress and strain components with respect to laminate axes (see Fig. 1). The stress strain relations after usual transformations for a typical layer L with respect to laminate axes can be found in Kant and Kommineni (1992).

Then the laminate constitutive relations can be obtained in compact form as

$$\begin{bmatrix} \boldsymbol{N} \\ \boldsymbol{M} \\ \boldsymbol{Q}_s \end{bmatrix} = \begin{bmatrix} \boldsymbol{D}_m & \boldsymbol{D}_c & 0 \\ \boldsymbol{D}_c^t & \boldsymbol{D}_b & 0 \\ 0 & 0 & \boldsymbol{D}_s \end{bmatrix} \begin{bmatrix} \bar{\boldsymbol{\varepsilon}}_m \\ \bar{\boldsymbol{\varepsilon}}_b \\ \bar{\boldsymbol{\varepsilon}}_s \end{bmatrix} \tag{6a}$$

or symbolically

$$\bar{\boldsymbol{\sigma}} = \boldsymbol{D}\,\bar{\boldsymbol{\varepsilon}} \tag{6b}$$

where $\boldsymbol{N}^t = [N_x, N_y, N_{xy}, N_x^*, N_y^*, N_{xy}^*]$ $\boldsymbol{M} = [M_x, M_y, M_{xy}, M_x^*, M_y^*, M_{xy}^*]$ $\boldsymbol{Q} = [Q_x, Q_y, Q_x^*, Q_y^*, S_x, S_y]$ and the stiffness coefficient matrices $\boldsymbol{D}_m$, $\boldsymbol{D}_c$, $\boldsymbol{D}_b$, $\boldsymbol{D}_s$ are defined as follows

$$\boldsymbol{D}_m = \sum_{L=1}^{NL} \begin{bmatrix} \boldsymbol{Q}_{ij}H_1 & \boldsymbol{Q}_{ij}H_3 \\ \boldsymbol{Q}_{ij}H_3 & \boldsymbol{Q}_{ij}H_5 \end{bmatrix} \; ; \; \boldsymbol{D}_c = \sum_{L=1}^{NL} \begin{bmatrix} \boldsymbol{Q}_{ij}H_2 & \boldsymbol{Q}_{ij}H_4 \\ \boldsymbol{Q}_{ij}H_4 & \boldsymbol{Q}_{ij}H_6 \end{bmatrix}$$

$$\boldsymbol{D}_b = \sum_{L=l}^{NL} \begin{bmatrix} \boldsymbol{Q}_{ij}H_3 & \boldsymbol{Q}_{ij}H_5 \\ \boldsymbol{Q}_{ij}H_5 & \boldsymbol{Q}_{ij}H_7 \end{bmatrix} \; ; \; \boldsymbol{D}_s = \sum_{L=l}^{NL} \begin{bmatrix} \boldsymbol{Q}_{lm}H_1 & \boldsymbol{Q}_{lm}H_3 & \boldsymbol{Q}_{lm}H_2 \\ \boldsymbol{Q}_{lm}H_3 & \boldsymbol{Q}_{lm}H_5 & \boldsymbol{Q}_{lm}H_4 \\ \boldsymbol{Q}_{lm}H_2 & \boldsymbol{Q}_{lm}H_4 & \boldsymbol{Q}_{lm}H_3 \end{bmatrix} \tag{6c}$$

In the above relations $i, j = 1, 2, 3$ and $l, m = 4, 5$ and $H_k = \frac{1}{k}(z_{L+1}^k - z_L^k)$, $k = 1, 2, 3, 4, 5, 6, 7$ and NL is the number of layers and $\bar{\boldsymbol{\varepsilon}} = (\bar{\boldsymbol{\varepsilon}}_m^t, \bar{\boldsymbol{\varepsilon}}_b^t, \bar{\boldsymbol{\varepsilon}}_s^t)^t$ represents the mid-plane membrane, bending and shear strain components respectively and are defined as follows

$$\boldsymbol{\varepsilon}_m = \begin{bmatrix} \frac{\partial u_o}{\partial x} + \frac{1}{2}[\frac{\partial w_o}{\partial x}]^2 \\ \frac{\partial v_o}{\partial y} + \frac{1}{2}[\frac{\partial w_o}{\partial y}]^2 \\ \frac{\partial v_o}{\partial x} + \frac{\partial u_o}{\partial y} + \frac{\partial w_o}{\partial x}\frac{\partial w_o}{\partial y} \\ \frac{\partial u_o^*}{\partial x} \\ \frac{\partial v_o^*}{\partial y} \\ \frac{\partial v_o^*}{\partial x} + \frac{\partial u_o^*}{\partial y} \end{bmatrix} \; ; \; \boldsymbol{\varepsilon}_b = \begin{bmatrix} \frac{\partial \theta_x}{\partial x} \\ \frac{\partial \theta_y}{\partial y} \\ \frac{\partial \theta_y}{\partial x} + \frac{\partial \theta_x}{\partial y} \\ \frac{\partial \theta_x^*}{\partial x} \\ \frac{\partial \theta_y^*}{\partial y} \\ \frac{\partial \theta_y^*}{\partial x} + \frac{\partial \theta_x^*}{\partial y} \end{bmatrix} \; ; \; \boldsymbol{\varepsilon}_s = \begin{bmatrix} \theta_x + \frac{\partial w_o}{\partial x} \\ \theta_y + \frac{\partial w_o}{\partial y} \\ 3\theta_x^* \\ 3\theta_y^* \\ 2u_o^* \\ 2v_o^* \end{bmatrix} \tag{7a}$$

and

$$\bar{\boldsymbol{\varepsilon}}^t = (\bar{\boldsymbol{\varepsilon}}_m^t, \bar{\boldsymbol{\varepsilon}}_b^t, \bar{\boldsymbol{\varepsilon}}_s^t) \tag{7b}$$

The discretization details of this element are available in Kommineni (1992). The strain displacement relations can be written as follows (eg. Zienkiewicz 1977).

$$\bar{\boldsymbol{\varepsilon}} = (\boldsymbol{B}_o + \frac{1}{2}\boldsymbol{B}_{nl})\,\boldsymbol{a}$$

$$\delta\bar{\boldsymbol{\varepsilon}} = (\boldsymbol{B}_o+\boldsymbol{B}_{nl})\,\delta\boldsymbol{a}$$
$$\delta\bar{\boldsymbol{\sigma}} = \boldsymbol{D}\,\boldsymbol{B}\,\delta\boldsymbol{a} \tag{8}$$

where $\boldsymbol{B}_o$ is the linear strain displacement matrix and $\boldsymbol{B}_{nl}$ non-linear strain displacement matrix which is linearly dependent upon the nodal displacement $\boldsymbol{a}$ i. e., $\boldsymbol{a}^t=(\boldsymbol{d}_1^t, \boldsymbol{d}_2^t, \boldsymbol{d}_3^t, \cdots, \boldsymbol{d}_{NN}^t)$, $\boldsymbol{B}$ is total strain displacement matrix and non-zero elements of $\boldsymbol{B}$ matrix corresponding to membrane, flexure and shear terms are as follows.

Membrane and flexure terms :

$$B_{1,1}=B_{3,2}=B_{4,6}=B_{6,7}=B_{7,4}=B_{9,5}=B_{10,8}=B_{12,9}=\frac{\partial N_i}{\partial x}$$
$$B_{2,2}=B_{3,1}=B_{5,7}=B_{6,6}=B_{8,5}=B_{9,4}=B_{11,9}=B_{12,8}=\frac{\partial N}{\partial y}$$
$$B_{1,3}=\frac{\partial w_o}{\partial x}\frac{\partial N_i}{\partial x}\,;\,B_{2,3}=\frac{\partial w_o}{\partial y}\frac{\partial N_i}{\partial y}\,;\,B_{3,3}=\frac{\partial w_o}{\partial x}\frac{\partial N_i}{\partial y}+\frac{\partial w_o}{\partial y}\frac{\partial N_i}{\partial x}$$

Shear terms:

$$B_{1,3}=\frac{\partial N_i}{\partial x}\,;\,B_{2,3}=\frac{\partial N_i}{\partial y}\,;\,B_{1,4}=B_{2,5}=N_i\,;$$
$$B_{3,8}=B_{4,9}=3N_i\,;\,B_{5,6}=B_{6,7}=2N_i \tag{9}$$

The expressions for the variation of strain energy, kinetic energy and work done by the external loads can be written as

$$\delta U = \delta\boldsymbol{a}^t\,(\int_A \boldsymbol{B}^t\,\bar{\boldsymbol{\sigma}}\,dx\,dy)$$
$$\delta E = -\delta\boldsymbol{a}^t\,(\int_A \boldsymbol{N}^t\,\bar{\boldsymbol{m}}\boldsymbol{N}\,dx\,dy)\,\ddot{\boldsymbol{a}}$$
$$\delta W = \delta\boldsymbol{a}^t\,(\int_A \boldsymbol{N}^t\,\boldsymbol{q}\,dx\,dy) \tag{10}$$

where $\boldsymbol{a}$, $\ddot{\boldsymbol{a}}$, $\boldsymbol{q}$ respectively defined as nodal displacement, acceleration and load vectors. $\boldsymbol{N}$ is defined as shape function matrix i. e., $(\boldsymbol{N}_1, \boldsymbol{N}_2, \cdots, \boldsymbol{N}_{NN})$. Substituting Eq. 10 in Eq. (4) and simplifying the equation we get

$$\int_{t_1}^{t_2} \delta\boldsymbol{a}^t\,(\boldsymbol{M}+\ddot{\boldsymbol{a}}+\boldsymbol{P}(a, t)-\boldsymbol{F}(t))\,dt = 0 \tag{11}$$

Since this relation is valid for every virtual displacement $\delta\boldsymbol{a}$ then

$$\boldsymbol{M}\ddot{\boldsymbol{a}}+\boldsymbol{P}(a, t) = \boldsymbol{F}(t) \tag{12}$$

which is the global equation of motion, where $\boldsymbol{M}$ is the global mass matrix, $\boldsymbol{P}(a, t)$ and $\boldsymbol{F}(t)$ are respectively global internal and external load vectors at time t.

$$\boldsymbol{P}(a, t)=\int_A \boldsymbol{B}^t\,\bar{\boldsymbol{\sigma}}\,dx\,dy \tag{13}$$

The mass matrix $\boldsymbol{M}$ in the Eq. (12) is given by

$$M = \int_A N^t \, \overline{\boldsymbol{m}} \, N \, dA$$

$$\text{where} \quad \overline{\boldsymbol{m}} = \begin{bmatrix} I_1 & & & & & & & & O \\ & I_1 & & & & & & & \\ & & I_1 & & & & & & \\ & & & I_2 & & & & & \\ & & & & I_2 & & & & \\ & & & & & I_3 & & & \\ & & & & & & I_3 & & \\ & & & & & & & I_4 & \\ O & & & & & & & & I_4 \end{bmatrix}$$

in which I_1, I_2, I_3, I_4 are normal inertia, rotary inertia and respective higher order inertia terms. These are given by

$$(I_1, I_2, I_3, I_4) = \sum_{L=1}^{NL} \int_{z_L}^{z_{L+1}} (1, z^2, z^4, z^6) \, \rho^L \, dz$$

and ρ^L is material density of the L^{th} layer. These diagonalized terms are scaled with respect to translation (but not rotation) terms in such away that the total mass is conserved (see Mallikarjuna and Kant 1990).

The numerical solution to the ordinary differential equation (12) is obtained using an explicit central difference scheme. The advantage of using the central difference method should now become apparent. Since no internal force vector and mass matrices of the complete element assemblage need to be calculated, the solution can essentially be carried out on the element level and relatively little high speed storage is required. Further the usual iterative solution procedure for the solution of a non-linear system of equations is completely avoided since the solution in the time domain is obtained here for each degree of freedom independently. Using the central difference scheme, systems of very large order equations can be solved efficiently. This scheme can be written as,

$$\boldsymbol{a}^{n+1} = \boldsymbol{M}^{-1} \times (\Delta t)^2 \, (-\boldsymbol{P}^n + \boldsymbol{F}^n) - \boldsymbol{a}^{n-1} - 2\boldsymbol{a}^n \tag{14}$$

where superscripts $n-1$, n, $n+1$ stand for three successive time stages and Δt is the time step length. The main advantage of this approach is that when $\boldsymbol{M}$ is diagonal, the computations at each step is trivial.

Since there is no estimate on the time step for the non-linear analysis is available in literature, in the present investigation, the initial estimate is calculated using the modified form of Tsui and Tong (1971) by Mallikarjuna and Kant (1990).

$$\Delta t \leq \Delta t_{cri} = \Delta x \left[\frac{\rho(1-\nu^2)/E_2 R}{\{2 + (1-\nu)\,(\pi^2/12)\,(1+1.5(\Delta x/h))^2\}} \right]^{\frac{1}{2}} \tag{15}$$

in which Δx is the smallest distance between adjacent nodes in any quadrilateral element used. E_1 and E_2 are the Youngs modulii in 1 and 2 directions respectively (see Fig. 1) and $R = E_1/E_2$. The final estimate is done after carrying out the convergence checks in order to save the computational costs.

3. Numerical results

In the present study the nine node quadrilateral isoparametric element is employed. Due to the biaxial symmetry of the problems discussed only one quadrant of the laminate is analyzed with a 2×2 mesh except for angle-ply laminates which are analyzed by considering full laminates with a 4×4 mesh. In all the numerical computations, the selective integration rule is employed. The element mass matrix is evaluated using a 3×3 Gauss-quadrature rule. For numerical computations two programs, a first order shear deformation theory (FOST) and a higher order shear deformation theory (HOST) with five and nine degrees of freedom per node respectively are developed. All the computations were carried out in a single precision on CDC Cyber 180/840 computer at Indian Institute of Technology, Bombay, India. All the stress values are evaluated at the Gauss points. The shear correction coefficient used in first order shear deformation theory is assumed as 5/6.

In order to test the accuracy and efficiency of developed algorithm, and to investigate effects of transverse shear deformations, the following material property sets were used in obtaining the numerical results.

Material set 1:

$$a=\sqrt{2},\quad b=1,\quad h=0.2,\quad \rho=1,\quad \nu=0.3 \quad \text{and} \quad E=1. \text{ (non-dimensional)}$$

Material set 2:

$$E_1=25E_2\ ;\quad G_{12}=G_{23}=G_{31}=0.5E_2\ ;\quad \rho=8\times10^{-6}\ N\ s^2/cm^4$$
$$\nu_{12}=0.25\ ;\quad E_2=2.1\times10^6\ N/cm^2\ ;\quad a=b=25\ cm\ ;\quad h=5\ cm$$

Material set 3:

Middle layer $E=19.2\times10^6\ psi$; $\nu=0.24$; $E_z=1.56\times10^6\ psi$
$G_z=0.82\times10^6\ psi$; $\nu_z=0.24$ and $\rho=0.00013\ lb\ s^2/in^4$
Outer layers $E=20.83\times10^6\ psi$; $\nu=0.44$; $E_z=10.0\times10^6\ psi$
$G_z=3.7\times10^6\ psi$; $\nu_z=0.44$ and $\rho=0.00013\ lb\ s^2/in^4$
Geometry $a/h=10$; $h=1$; $h_1=h_3=h_2/2$

Material set 4:

$$E=100\ psi\ ;\quad \nu=0.3\ ;\quad \rho=10\ lb\ s^2/in^4,$$
$$a=10\ in\ ;\quad b=1\ in\ ;\quad h=1\ in\ ;\quad q_o=0.02\ lb/in^2$$

Material set 5:

$$E=7.031\times10^5\ kg/cm^2\ ;\quad \nu=0.25\ ;\quad \rho=2.547\times10^{-6}\ kg\ s^2/cm^4\ ;$$
$$a=b=243.8\ cm\ ;\quad h=0.635\ cm\ ;\quad q_o=4.882\times10^{-4}\ kg/cm^2\ (0\le t\le\infty)$$

Material set 6:

$$a=b=100\ cm,\quad h=10\ cm$$

Face sheets (Graphite/Epoxy prepreg system)

$$E_1=1.308\times10^7\ N/cm^2\ ;\quad E_2=1.06\times10^6\ N/cm^2\ ;\quad G_{12}=G_{13}=6\times10^5\ N/cm^2,$$

$$G_{23}=3.9\times10^{5}N/cm^{2}\ ;\quad \rho=1.58\times10^{-5}\ N\ s^{2}/cm^{4}\ ;\quad v_{12}=0.28$$

Thickness of each top stiff layer = 0.025 h
Thickness of each bottom stiff layer = 0.08125 h
Core (US Commercial al. honeycomb, 1/4 in cell size, .003 in foil)

$$G_{23}=1.772\times10^{4}\ N/cm^{2}\ ;\quad G_{13}=5.206\times10^{4}\ N/cm^{2}\ ;\quad \rho=1.009\times10^{-6}\ Ns^{2}/cm^{4}$$

Thickness of core = 0.6 h

The finite element displacement formulation developed in this paper is based entirely on assumed displacement functions and thus, only displacement boundary conditions are required to be specified. The boundary conditions corresponding to the present higher order formulation are specified in Table 1 for different types of supports used in the present investigation.

Table 1 Boundary conditions

Type	$x=0$ / $x=a$	$x=a/2$	$y=0$ / $y=b$	$y=b/2$
$S1$	$v_o=0\ \ v_o^*=0$ $\theta_y=0\ \ \theta_y^*=0$ $w_o=0$	$u_o=0\ \ u_o^*=0$ $\theta_x=0\ \ \theta_x^*=0$	$u_o=0\ \ u_o^*=0$ $\theta_x=0\ \ \theta_x^*=0$ $w_o=0$	$v_o=0\ \ v_o^*=0$ $\theta_y=0\ \ \theta_y^*=0$
$S2$	$u_o=0\ \ u_o^*=0$ $\theta_y=0\ \ \theta_y^*=0$ $w_o=0$	$u_o=0\ \ u_o^*=0$ $\theta_x=0\ \ \theta_x^*=0$	$v_o=0\ \ v_o^*=0$ $\theta_x=0\ \ \theta_x^*=0$ $w_o=0$	$v_o=0\ \ v_o^*=0$ $\theta_y=0\ \ \theta_y^*=0$
$S3$	$u_o=0\ \ u_o^*=0$ $v_o=0\ \ v_o^*=0$ $\theta_y=0\ \ \theta_y^*=0$ $w_o=0$	$u_o=0\ \ u_o^*=0$ $\theta_x=0\ \ \theta_x^*=0$	$u_o=0\ \ u_o^*=0$ $v_o=0\ \ v_o^*=0$ $\theta_x=0\ \ \theta_x^*=0$ $w_o=0$	$v_o=0\ \ v_o^*=0$ $\theta_y=0\ \ \theta_y^*=0$
C	$u_o=0\ \ u_o^*=0$ $v_o=0\ \ v_o^*=0$ $\theta_x=0\ \ \theta_x^*=0$ $\theta_y=0\ \ \theta_y^*=0$ $w_o=0$	$u_o=0\ \ u_o^*=0$ $\theta_x=0\ \ \theta_x^*=0$	$u_o=0\ \ u_o^*=0$ $v_o=0\ \ v_o^*=0$ $\theta_x=0\ \ \theta_x^*=0$ $\theta_y=0\ \ \theta_y^*=0$ $w_o=0$	$v_o=0\ \ v_o^*=0$ $\theta_y=0\ \ \theta_y^*=0$

The corresponding boundary conditions for the first order shear deformation theory is simply obtained by omitting the higher order starred (*) displacement quantities. For example there are nine displacement quantities required to be specified at $x=0$, a for C type of boundary conditions in this higher order formulation (HOST), whereas in first order formulation (FOST) the corresponding boundary conditions shall be five only. The boundary condition types $S1$, $S2$ and $S3$ have been especially chosen in order to compare our results with those of other authors. Incidentally, the $S1$ type condition corresponds to the usual diaphragm type of simple support. The edge conditions, which have been derived in a variationally consistent manner in the present higher order theory may not appear so (except in the case of fully clamped edge specified by C), because, in any way, the natural boundary conditions can not be prescribed in the displacement based finite element method.

The results that are to be discussed are grouped in to two categories, viz.; 1. Linear analysis and 2. Non-linear analysis

3.1. Linear analysis

3.1.1. Isotropic plate subjected to patch load at the center

In order to validate the present theory, a problem for which analytical solution exists has been solved. The problem consists of a simply supported ($S1$) rectangular plate with geometry and material properties as per material set 1 subjected to an uniform pulse load on a square (side$=0.4b$) area at the center of plate. A non-uniform 4×4 mesh of elements was employed. A comparison of non-dimensional center deflection and bending moments obtained by present theory and Reismann and Lee (1969) is shown in Figs 2a and 2b. The classical plate theory (i.e., not accounting for transverse shear strains) is also given in Figures to show the influence of shear deformation on the results. The present finite element solution for the center deflection is in excellent agreement with a thick plate analytical solution. Since the bending mo–

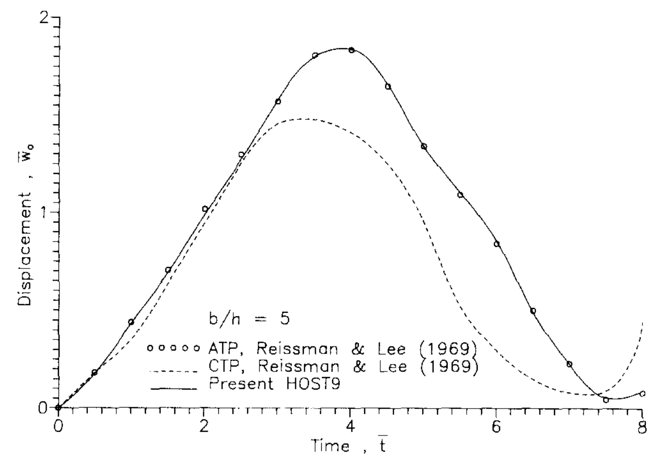

(a) Central displacement vs. time for a simply supported($S1$)

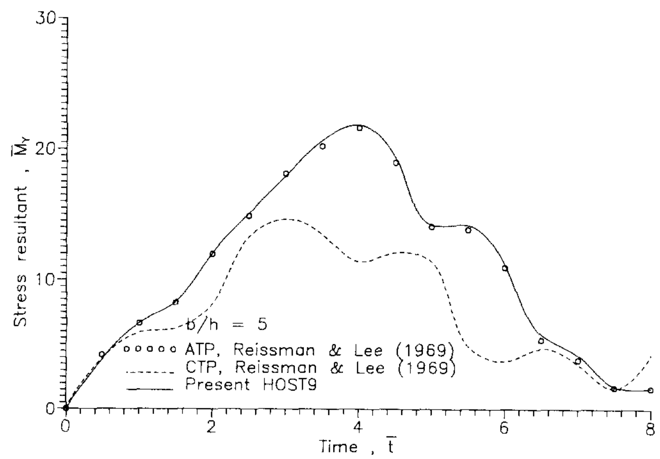

(b) Stress resultant vs. time for a simply supported($S1$)

Fig. 2 Rectangular isotropic plate under suddenly applied patch load ($q_o=1$, $\Delta t=0.02$ sec) ments in the present study were calculated at the Gauss points, it is not expected to match exactly with that at the center of the plate. The non-dimensional quantities used are as follows

$$\bar{t} = (t/b)(\sqrt{E/\rho}\,) ; \quad \overline{w}_o\left[\frac{w_o Eah}{q_o b^3}\right]; \quad \overline{M}=\left[\frac{12aM_y}{q_o b^2 h^2}\right] \tag{16}$$

3.1.2. Cross-ply laminate

A two layer cross-ply (0°/90°) square laminate with geometry and material properties as per material set 2 and subjected to a suddenly applied sinusoidal distributed load is considered. For the same problem Reddy (1982) presented a closed-form solution with a first order shear deformation theory. The present solution and the closed-form solution for central deflection, central normal stress and corner in-plane shear stress are compared in Fig. 3 and Table

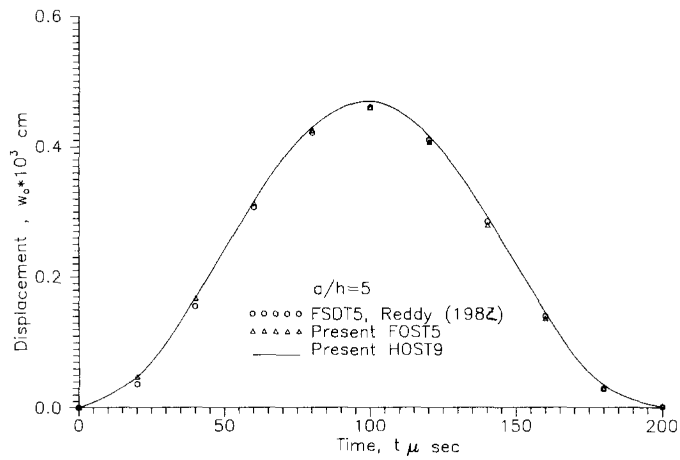

Fig. 3 Central displacement vs. time for a simply supported($S1$) square cross-ply (0°/90°) laminate under suddenly applied sinusoidal transverse load (q_o=10 psi, Δt=0.5 μ sec)

Table 2 Comparison of stresses obtained in the present study with those obtained by the Reissner-Mindlin's plate theory for a two layer square cross-ply (0°/90°) laminate under suddenly applied sinusoidal transverse load.
Δt=0.25 μ sec (Linear analysis)

Time μ sec	Normal stress σ_x N/cm^2			Shear stress τ_{xy} N/cm^2		
	FOST5*	Present$^+$	%Differ	FOST5*	Present$^+$	%Differ
20	28.48	39.745	28.34	1.611	2.594	37.90
40	113.60	126.70	10.34	8.506	10.525	19.18
60	227.20	241.01	5.73	16.470	19.364	14.95
80	319.10	324.69	1.72	23.850	27.030	11.76
100	357.80	357.22	0.16	26.270	29.103	9.73
120	323.10	314.47	2.74	24.120	26.069	7.48
140	233.00	223.93	4.05	17.050	18.103	5.82
160	119.60	111.59	7.18	8.848	8.988	1.56
180	30.40	28.06	8.34	2.029	1.947	4.21

* Closed form solution from Reddy (1982)
+ Present HOST9

2. From these results, it is clear that Reissner-Mindlin theory under predict stresses for layered composite plates.

3.1.3. **Layered orthotropic plate**

To validate the present theory further, another problem for which closed-form higher order solution exists has been solved. For this purpose, a three layer (thickness of each outer layer equals half of the thickness of middle layer) simply supported ($S1$) orthotropic laminate with geometry and material properties as per material set 3 and subjected to a step, a triangular

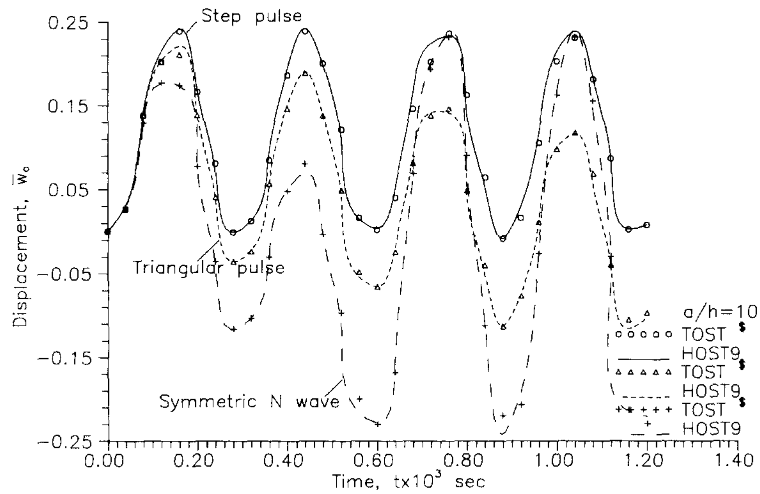

Fig. 4 Central displacement vs. time for a simply supported(S1) square orthotropic 3 layered plate (q_0 =4500 psi, $\Delta t = 1$ μ sec). ($ indicates values given by Nosier and Reddy 1991)

and a symmetric N wave with durations $0.002sec$, $0.001sec$ and $0.001sec$ respectively is considered. The present responses are compared with a closed form higher order solution responses given by Nosier adn Reddy (1991) and are presented in Fig. 4. The non-dimensional quantity for representing displacement is

$$\overline{w}_o = [\frac{w_o}{h}] \tag{17}$$

The present results exactly match with closed-form third order solution given by Nosier and Reddy (1991).

3.2. *Non-linear analysis*

3.2.1. **Infinite long plate**

To validate the present theories in non-linear context, a clamped (C) isotropic plate, which is infinitely extended in one direction is modelled, invoking symmetry by 5 plate bending elements. The loading is a suddenly applied uniformly distributed pulse load and geometry and material properties are as per material set 4. The present results are compared with Pica and Hinton (1980) and are presented in Fig. 5a. The present results exactly match with the Pica & Hinton (1980) results. This validates the present formulation in non-linear context.

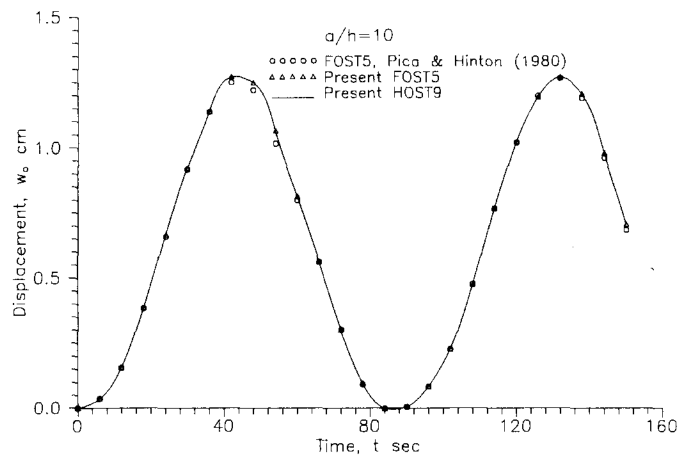

Fig. 5a Central displacement vs. time for an infinite long isotropic plate under suddenly applied uniform pulse load (q_o=0.02 kg/cm^2, Δt=0.06 sec)

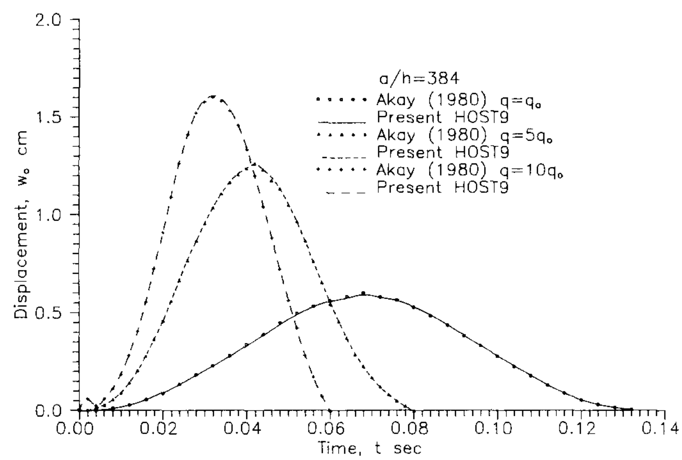

Fig. 5b Central displacement vs. time for a simply supported(S3) square plate subjected to uniform pulse load (q_o=4.882$\times$10^{-4} kg/cm^2, Δt=0.5 μ sec)

3.2.2. Isotropic plate

A simply supported (S3) isotropic plate with geometry and material properties as per material set 5 and subjected to a uniform pulse load is considered. This problem was solved by Akay (1980) using four noded isoparametric quadrilateral mixed finite elements with 2×2 mesh in a quadrant with a time increment Δt=0.005*sec*. In the present study, only one element in a quadrant is used. The same problem with same material properties is also solved by Bayles et al. (1973) who developed a finite difference scheme for dynamic von Karman equations, and employed an 8×8 mesh with time increment of Δt=0.0005*sec*.

The variation of center transverse deflection with respect to time for different load magnitudes q_o, $5q_o$, $10q_o$ is shown in Fig. 5b. The effect of load magnitude on non-linear response is clearly seen in the plots. It is observed that the nine noded quadrilateral isoparametric element is capable of rendering good accuracy with relatively coarser mesh.

3.2.3. **Convergence study**

In order to investigate the numerical convergence of the transient behaviour of the element, two simply supported (S1) 0° orthotropic and (0°/90°) cross-ply laminates with geometry and material properties as per material set 2 and with a suddenly applied uniform pulse load were analyzed. Tables 3 and 4 present the center deflection and normal stress values for different meshes and time steps. From the results it is found that Eq. (15) is valid to estimate the initial time step in non-linear analysis of fibre reinforced composite laminates.

Table 3 Convergence of center deflection and stress values for different time steps for an orthotropic laminate (Non-linear analysis)

Time μ sec	Δt μsec →	0.25			0.5	0.6668
	quantity	2×2	3×3	4×4	2×2	2×2
40	$\overline{w}_o$	0.45844	0.4561	0.4558	0.46152	0.4638
	$\hat{\sigma}_x$	25.61786	25.0786	24.9702	25.81500	25.9710
80	$\overline{w}_o$	0.96218	0.9608	0.9603	0.96173	0.9614
	$\hat{\sigma}_x$	53.07500	51.8880	51.0643	53.08200	53.0655
120	$\overline{w}_o$	0.42290	0.4265	0.4268	0.42084	0.4191
	$\hat{\sigma}_x$	21.25360	20.2035	19.9429	21.14500	21.0012
160	$\overline{w}_o$	-0.06468	-0.0632	-0.0617	-0.06494	-0.0652
	$\hat{\sigma}_x$	-3.88702	-3.5708	-3.2046	-3.87905	-3.9083
200	$\overline{w}_o$	0.60674	0.5895	0.5852	0.60937	0.6119
	$\hat{\sigma}_x$	35.15710	32.7238	32.0107	35.23810	35.3381

Table 4 Convergence of center deflection and stress values for different time steps for a two layer cross-ply (0°/90°) square laminate (Non-linear analysis)

Time μ sec	Δt μsec →	0.25			0.5	0.6668
	quantity	2×2	3×3	4×4	2×2	2×2
40	$\overline{w}_o$	0.48958	0.4872	0.4871	0.49312	0.4957
	$\hat{\sigma}_x$	22.31670	21.3240	21.3240	22.48700	22.5964
80	$\overline{w}_o$	1.10249	1.1060	1.1013	1.10275	1.1029
	$\hat{\sigma}_x$	52.90360	52.4060	51.2036	52.91070	52.8881
120	$\overline{w}_o$	0.64812	0.6846	0.6909	0.64504	0.6424
	$\hat{\sigma}_x$	31.02140	32.1650	33.1845	30.88810	30.7821
160	$\overline{w}_o$	0.01650	0.0095	0.0107	0.01630	0.0161
	$\hat{\sigma}_x$	0.55830	0.5058	0.6322	0.54785	0.5772
200	$\overline{w}_o$	0.35451	0.3251	0.3211	0.35720	0.3599
	$\hat{\sigma}_x$	15.69762	13.0770	12.6036	15.80950	15.8857

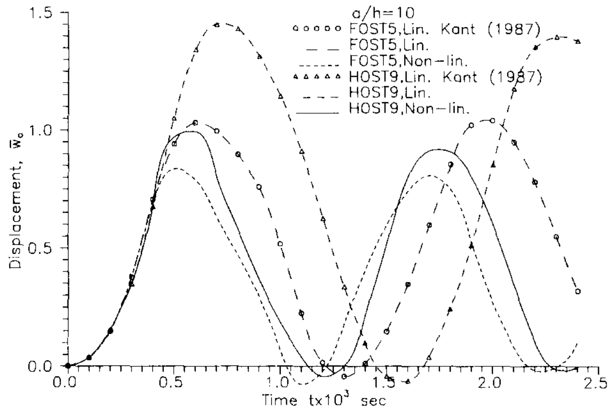

(a) Central displacement vs. time

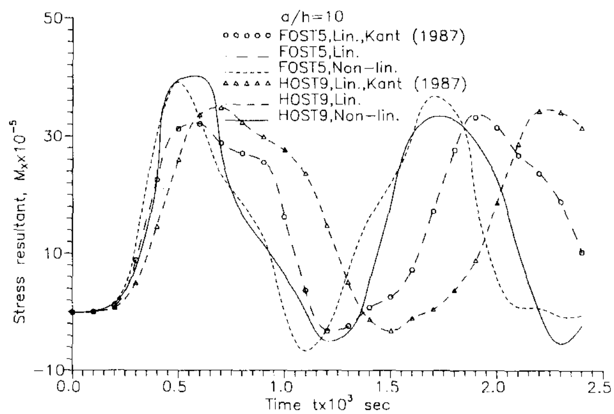

(b) Bending moment vs. time

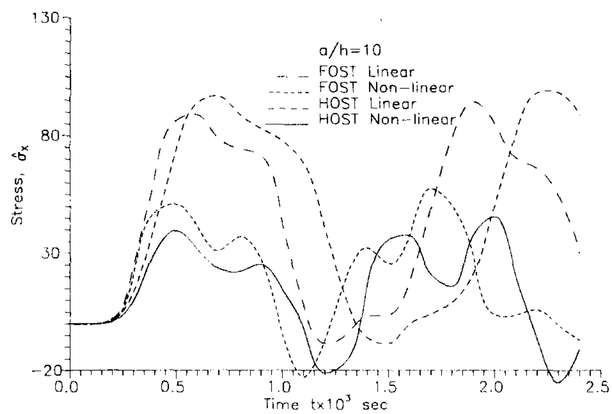

(c) Stress vs. time

Fig. 6 A clamped(C) angle-ply sandwich laminate (0°/45°/90°/CORE/90°/45°/30°/0°) under suddenly applied uniform transverse load (q_o = 5000 N/cm², Δt = 5 μ sec)

3.2.4. **Sandwich laminate**

A clamped (C) angle-ply (0°/45°/90°/CORE/90°/45°/30°/0°) sandwich laminate with geometry and material properties as per material set 6 subjected to a suddenly applied uniform pulse load is considered. The plots for displacement, stress resultant and stresses vs. time respectively are presented in Figs 6a-6c for linear and geometrically non-linear analyses by using first order shear deformation theory as well as higher order shear deformation theory along with corresponding linear analysis results of Kant (1987). The non-dimensional quantities used are defined as follows

$$\overline{w}_o = \frac{w_o}{h}; \quad \hat{\sigma}_x = \frac{\sigma_x}{E_2}\left[\frac{a}{h}\right]^2 \tag{18}$$

The present linear results exactly match with Kant (1987). From the results it is confirmed that even at $a/h = 10$ first order shear deformation theory under predicts displacements as well as stresses in linear as well as non-linear analyses. It is also to be noted that due to non-linearity the amplitude of vibration reduces when compared with linear responses.

4. Conclusions

Numerical results of the linear and geometrically non-linear analyses of isotropic, orthotropic and layered composite and sandwich laminates are presented. The simple C° isoparametric formulation of an assumed higher order displacement model employed here is stable and accurate in predicting the linear and geometrically non-linear transient responses of composite and sandwich laminates. In contract to first order shear deformation theory, the present theory does not require the usual shear correction factors generally associated with first order shear deformation theory. The present finite element results in linear and geometrically non-linear analyses agree very well with the available analytical and other finite element solutions in literature. The simplifying assumptions made in classical plate theory (CPT) and first order shear deformation theory (FOST5) are reflected by high percentage of errors especially in the predictions of sandwich laminates. It is believed that the refined shear deformation theory presented here-in is essential for predicting accurate responses of sandwich laminates. The present results of linear and geometrically non-linear analyses of sandwich laminates should serve as reference results for future investigations.

Acknowledgements

Partial support of this research by the Aeronautics Research and Development Board, Ministry of Defence, Government of India through its Grant Nos. Aero/RD-134/100/10/88-89/518 and Aero/RD-134/100/10/88-89/534 is gratefully acknowledged.

References

Akay, H. U. (1980), "Dynamic large deflection analysis of plates using mixed finite elements", *Comput. Struc.*, **11**, 1-11.

Bayles, D. J., Lowery, R. L. and Bovd, D. E. (1973), "Non-linear vibrations of rectangular plates", *ASCE, J. Struct. Division,* **99**, 853-864.

Hinton, E., Rock, T. A. and Zienkiewicz, O. C. (1976), "A note on mass lumping and related processes in the finite element method", *Earthquake Engng Struct. Dynamics,* **4,** 245-249.

Hinton, E. (1976), "The dynamic transient analysis of axisymmetric circular plates by the finite method", *J. Sound Vib.,* **46,** 465-472.

Kant, T. (1987), "Transient dynamics of fibre reinforced composite plates", *Research Project Report, Aeronautics Research and Development Board,* Ministry of Defence, Government of India, Aero/RD-134/100/10/83-84/362.

Kant, T. and Kommineni, J. R. (1992), "C^0 Finite element geometrically non-linear analysis of fibre reinforced composite and sandwich laminates based on a higher order theory", *Comput. Struct.,* **45,** 511-520.

Kommineni, J. R. (1992), "Geometric and material non-linear static and dynamic analyses of composite and sandwich plates and shells with a refined", *Ph. D. Thesis,* Department of Civil Engineering, Indian Institute of Technology, Bombay.

Mallikarjuna and Kant, T. (1990), "Finite element transient response of composite and sandwich plates with a refined higher order theory", *ASME, J. App. Mech.* **57,** 1084-1086.

Nosier, A. and Reddy, J. N. (1991), "A study of non-linear dynamic equation of higher order shear deformation plate theories", *Int. J. Non-Linear Mech.,* **26,** 233-249.

Pica, A. and Hinton, E. (1980), "Transient and pseudo transient analysis of Mindlin plates", *Int. J. Num. Meth. Engg.* **15,** 188-208.

Reddy, J. N. (1982), "On the solutions to forced motions of rectangular composite plates", *ASME, J. App. Mech.,* **49,** 403-408.

Reddy, J. N. (1983), "Geometrically non-linear transient analysis of laminated composite plates", *AIAA J.,* **21,** 621-629.

Reismann, H. and Lee, Y. (1969), "Forced motions of rectangular plates", in *Developments in Theoretical and Applied Mechanics* (D. Frederick, editor), Pergamon Press, New York, **4,** 3-18.

Tsui, T. Y. and Tong, P. (1971), "Stability of transient solutions of moderately thick plates by finite difference methods", *AIAA J.,* **9,** 2062-2063.

Zienkiewicz, O. C. (1977), *The Finite Element Method,* Third Edition, McGraw-Hill, London.